



Trans. Nonferrous Met. Soc. China 28(2018) 1571-1581

Transactions of Nonferrous Metals Society of China

www.tnmsc.cn



# Antibacterial activities and corrosion behavior of novel PEO/nanostructured ZrO<sub>2</sub> coating on Mg alloy

Mohammadreza DAROONPARVAR<sup>1,2</sup>, Muhamad Azizi MAT YAJID<sup>1</sup>, Rajeev KUMAR GUPTA<sup>2</sup>, Noordin MOHD YUSOF<sup>1</sup>, Hamid Reza BAKHSHESHI-RAD<sup>1,3</sup>, Hamidreza GHANDVAR<sup>1</sup>, Ehsan GHASEMI<sup>4</sup>

1. Department of Materials, Manufacturing and Industrial Engineering,

Faculty of Mechanical Engineering, Universiti Teknologi Malaysia, 81310 Johor Bahru, Johor, Malaysia;

2. Department of Chemical and Biomilecular Engineering, Corrosion Engineering Program,

The University of Akron, Akron, OH-44325, United States of America;

3. Advanced Materials Research Center, Department of Materials Engineering, Najafabad Branch, Islamic Azad University, Najafabad, Iran;

4. Department of Clinical Sciences, Faculty of Veterinary Medicine, University of Tehran, Tehran, Iran

Received 4 June 2017; accepted 23 October 2017

**Abstract:** Plasma electrolytic oxidation (PEO) was developed as a bond coat for air plasma sprayed (APS) nanostructure ZrO<sub>2</sub> as top coat to enhance the corrosion resistance and antibacterial activity of Mg alloy. Corrosion behavior and antibacterial activities of coated and uncoated samples were assessed by electrochemical tests and agar diffusion method toward *Escherichia coli* (*E. coli*) bacterial pathogens, respectively. The lowest corrosion current density and the highest charge transfer resistance, phase angle and impedance modulus were observed for PEO/nano-ZrO<sub>2</sub> coated sample compared with those of PEO coated and bare Mg alloys. Nano-ZrO<sub>2</sub> top coat which has completely sealed PEO bond coat is able to considerably delay aggressive ions transportation towards Mg alloy surface and significantly enhances corrosion resistance of Mg alloy in simulated body fluid (SBF) solution. Moreover, higher antibacterial activity was also observed in PEO/nano-ZrO<sub>2</sub> coating against bacterial strains than that of the PEO coated and bare Mg alloys. This observation was attributed to the presence of ZrO<sub>2</sub> nanoparticles which decelerate *E. coli* growth as a result of *E. coli* membranes.

Key words: Mg alloy; ceramics; coating materials; microstructure; scanning electron microscopy (SEM)

#### 1 Introduction

High chemical activity and poor corrosion resistance of Mg and its alloys limit their biomedical applications in corrosive environments. Corrosion resistance of Mg and its alloys can substantially be improved by protective coatings. Various conventional coating techniques were used to reduce the surface activity of Mg and its alloys [1–4]. Plasma electrolytic oxidation (PEO) method is considered as an eco-friendly method to produce hard ceramic complex coatings with inert ceramic-like composition, excellent bond strength and relatively high thickness on metal substrates [5–7]. However, coatings which have been made by the PEO method are generally porous and include many micro-defects. These defects are able to reduce the

surface quality of PEO coatings and can easily conduct electrolyte towards alloy surface during corrosion [8]. Hence, some post-treatments should be performed to seal the micro-pores of PEO coatings and increase their protection performance [9–12]. However, some sealing coatings (such as sol–gel, organic, conversion, polymer coatings) showed undesirable mechanical properties and considerable micro-defects which originated from solvent vaporization or insufficient filling of PEO micro-pores due to the presence of air in these pores [9].

Recently, corrosion, oxidation and wear resistances of magnesium alloys have considerably been increased by plasma sprayed multilayer coatings including ceramic top coatings and metallic bond coating (such as NiCrAlY bond coat) [13–18]. However, there is high standard electrochemical potential difference between the metallic bond coat (as noble coating) and Mg alloy (as anode).

Once, electrolyte reaches Mg alloy/NiCrAlY bond coat (as non-biocompatible coat) interface, a sever galvanic cell can be formed at this interface which eventually leads the coating separation from to substrate [4,14,16–18]. Hence, it is predicted that PEO as a biocompatible ceramic bond coat could supply dockage locations for molten ceramic droplets during plasma spraying and could considerably reduce the galvanic cell formation between coating and Mg alloy during corrosion. In this vision, air plasma spraying which is a low cost and straightforward method [19-22] will be used for spraying nano-ZrO2 coating as sealing top coat on PEO inert bond layer. Nanostructured ZrO2 coating consisting of bimodal structure and non-transformable tetragonal ZrO2 phases showed bioactivity in SBF solution [23]. However, a study on the corrosion behavior and antibacterial properties of PEO/ nanostructured ZrO2 coating on biodegradable Mg alloy could not be found in the literature. Hence, in the present microstructure, corrosion behavior research, antibacterial activities of PEO coated Mg alloy and PEO/nanostructured ZrO<sub>2</sub> coated Mg alloy were explored.

#### 2 Experimental

### 2.1 Preparation of specimens for PEO and APS processes

Mg alloy (0.018% Si, 0.021% Mn, 0.008% Al, 0.011% Fe, 1.008% Ca and Mg balance) cylindrical ingot with diameter of 25 mm and length of 200 mm was cut out to specimens with dimensions of 15 mm × 15 mm × 6 mm. The composition of PEO mixture electrolyte comprised 2 g/L KOH, 13 g/L Na<sub>2</sub>SiO<sub>3</sub> and 7 g/L NaAlO<sub>2</sub>, which was freshly prepared and swiftly used for PEO process. On the other hand, a stainless steel plate with dimensions of 60 mm  $\times$  120 mm  $\times$  2 mm was employed as a counter electrode. The current density was maintained at 2 A/cm<sup>2</sup>. Moreover, the applied voltage and preparation time were 350 V and 10 min, respectively for this PEO process. The temperature of the electrolyte was kept at 15-20 °C by a water cooling system. The duty cycle of pulsed DC power supply unit was 60%. In the meantime, a relatively high pulse frequency of 1000 Hz was chosen for this process.

Granulated nanostructure ZrO<sub>2</sub> powders [24–26] (plasma spray-able agglomerated micro-meter sized granules) were successfully prepared and deposited on the PEO coated samples using air plasma spray system (3 MB gun, Sulzer Metco) with the aid of compressed air during plasma spraying and optimized APS parameters [4,16,17,26].

### 2.2 Characterization, electrochemical measurements and antibacterial activity test

The surface morphology and cross section of the coated Mg alloys were seen under Hitachi S4160 field emission scanning electron microscopy machine. In the meantime, elemental analysis of the coated samples was performed by energy dispersive spectroscopy (EDS) method. Moreover, low-angle X-ray diffraction (XRD with Cu  $K_{\alpha}$  radiation, Rigaku D, Japan) was used to do phase analysis of treated and untreated Mg samples in  $2\theta$  (diffraction angle) range of  $20^{\circ}-90^{\circ}$ .

Potentiodynamic polarization test was performed using a PARSTAT 2263 advanced electrochemical system in SBF solution at a scan rate of 1.0 mV/s (at room temperature). A saturated calomel electrode (SCE) as the reference electrode, a platinum rod as the counter electrode and the sample as the working electrode formed the electrochemical cell. Moreover, the exposure area was 1 cm<sup>2</sup>. On the other hand, for the electrochemical impedance spectrum (EIS) test, scan frequency ranged from 1 Hz to 10<sup>5</sup> Hz with perturbation amplitude of 5 mV.

The antibacterial activity of the uncoated and coated samples against *Escherichia coli* PTCC 1330 (Gramnegative) bacteria was examined according to the disc diffusion antibiotic sensitivity [27]. In the present study, gentamicin discs for bacteria (10  $\mu$ g/disc) were used as reference.

#### 3 Results and discussion

## 3.1 Microstructural characterization of PEO and multilayered coatings on Mg alloy

Figure 1(a) demonstrates the cross-section morphology of PEO coated Mg alloy. There is a good integrity between multiphase composite PEO coating ((15±1) µm in thickness) and Mg alloy substrate. This integrity originated from the sintered interlocking during PEO process. PEO film generally shows a duplex structure consisting of an outer layer which is porous and an inner barrier layer which is completely dense [28,29].

Vertical micro pores which are present in the outer porous layer of PEO coating are internally obstructed by dense inner barrier layer of PEO coating (see Figs. 1(a), 1(b) and 2(a)). This phenomenon can be ascribed to the pores in the PEO layer which always give birth to discharge during coating process [30]. Moreover, higher pores density on the outer porous layer would lead to the increment of effective surface area of the PEO coating. Hence, corrosive solution can increasingly be adsorbed by the micro-pores of outer porous layer and can quickly infiltrate into the inner barrier layer. This phenomenon would eventually lead to the galvanic cell formation between Mg alloy and corrosive solution. It is interesting

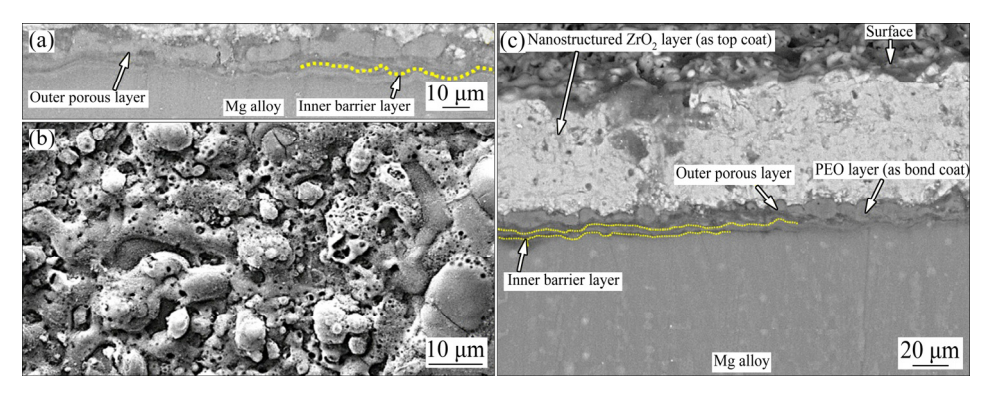


**Fig. 1** Cross-section FESEM image of PEO treated Mg alloy (a), surface morphology of PEO bond layer (high magnification) (b), and cross-section FESEM image of PEO/nanostructured ZrO<sub>2</sub> coated Mg alloy (c)

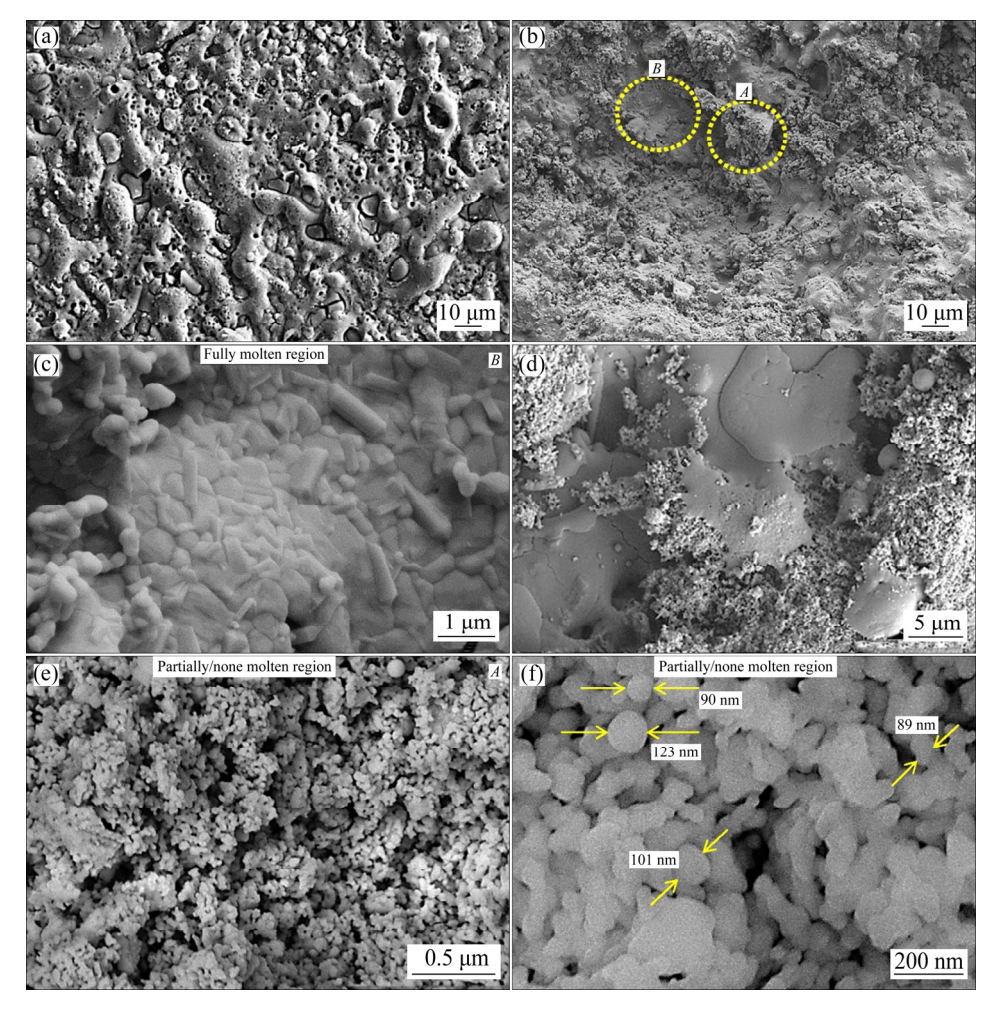


Fig. 2 Surface morphology of multiphase PEO coating (low magnification) (a) and surface morphologies of nanostructured ZrO<sub>2</sub> coating with compact and bimodal structure (b-f)

to note that sparking discharge, gas bubble and the considerably low Pilling–Bedworth (PB) ratio of Mg oxide to Mg substrate (about 0.81) would lead to the formation of micro-pores in the PEO coatings [9,31]. Hence, it is expected that corrosion resistance of PEO coated Mg alloy could be increased by sealing micro-pores of outer porous layer. This expectation could be performed by spraying nanostructured granulated ZrO<sub>2</sub> coating on multiphase PEO coating (as bond coat).

Figure 1(c) indicates the cross-section morphology of PEO/nanostructured  $ZrO_2$  coating ((60±5)  $\mu m$  in thickness) on Mg alloy. This system (coating) including inner barrier layer, outer porous layer and nanostructured  $ZrO_2$  layer is still bonded with Mg alloy after sever grinding and polishing for cross section characterization. Hence, it is speculated that there is suitable adhesion between coatings and Mg alloy.

There is nearly clear interface between the

nanostructured  $ZrO_2$  layer and multiphase PEO layer which indicates physical interlocking (integrity) between bond coat and nanostructured  $ZrO_2$  layer (as top coat). This observation could be ascribed to the infiltration of molten  $ZrO_2$  particles into the outer porous layer of PEO coating and followed by elimination of present air in the micro-pores during air plasma spraying (see Fig. 3(a)). Hence, nanostructured  $ZrO_2$  coating is able to considerably seal multiphase PEO layer.

As previously stated, Mg alloy surface (with high activity) can severely be oxidized under the direct effect of plasma flame (with high temperature). Moreover, thermal expansion coefficient (TEC) mismatch between ceramic coatings and Mg alloy was found to be very high. These phenomena led to the premature spallation of plasma sprayed ceramic coating from Mg surface after spraying process [14]. However, in this work, TEC mismatch between  $ZrO_2$  coating  $(7\times10^{-6}-8\times10^{-6} \text{ K}^{-1})$ and Mg alloy (26×10<sup>-6</sup> K<sup>-1</sup>) was significantly reduced by using an inert multiphase PEO layer (MgO:  $12.6 \times 10^{-6} \text{ K}^{-1}$ , MgAl<sub>2</sub>O<sub>4</sub>:  $7.5 \times 10^{-6} \text{ K}^{-1}$ , MgSiO<sub>2</sub>:  $6.5 \times 10^{-6} \,\mathrm{K}^{-1}$ ) as bond coat [13,32,33]. Hence, slightly thick multiphase PEO layer could be able to preserve Mg surface from sever oxidation during APS (with the aid of compressed air) and would prevent sprayed ceramic coating detachment from Mg alloy after spraying and its cooling down to ambient temperature (see Fig. 1(c)).

Figures 1(b) and 2(a) indicate surface morphology of PEO layer which is rough and porous. It is assumed

that outer porous layer of PEO coating could supply dockage locations for molten ZrO<sub>2</sub> droplets during plasma spraying.

Nanostructured ZrO<sub>2</sub> coating surface (Fig. 2(b)) showed less pinholes, voids and micro-cracks compared to PEO layer (Fig. 2(a)). This case is mainly related to the compactness of the nanostructure [34-39]. Plasma sprayed nanostructure ZrO2 coating showed a bi-model structure (see Figs. 2(b)–(f)) which was also observed by the previous investigators [14,17,24]. This structure includes partially/none molten regions (nano-regions (A)) (Figs. 2(e) and 2(f)) which are surrounded by fully molten regions (Figs. 2(b), 2(c)(B) and 2(d)). Thus, it is predicted that nanostructured ZrO<sub>2</sub> coating with bi-model and nearly compact structure could remarkably enhance the corrosion resistance and biocompatibility of multiphase PEO coated Mg alloy in SBF solution. It was reported that the presence of nano-regions on the coating surface would lead to the increment of biocompatibility of biomaterials [13,23,35].

The existence of Zr and O elements in the ZrO<sub>2</sub> coating and also the presence of Si, Al, Mg and O elements in the multiphase PEO layer as well as attendance of Mg and Ca elements in Mg-1%Ca alloy can easily be observed in the EDX mapping (see Figs. 3(a)-(f)) from cross section of multilayered coated Mg alloy. Moreover, the EDX area from surface of coatings proved the presence of Zr and O elements in the ZrO<sub>2</sub> coating and also the existence of Si, Al, Mg and O

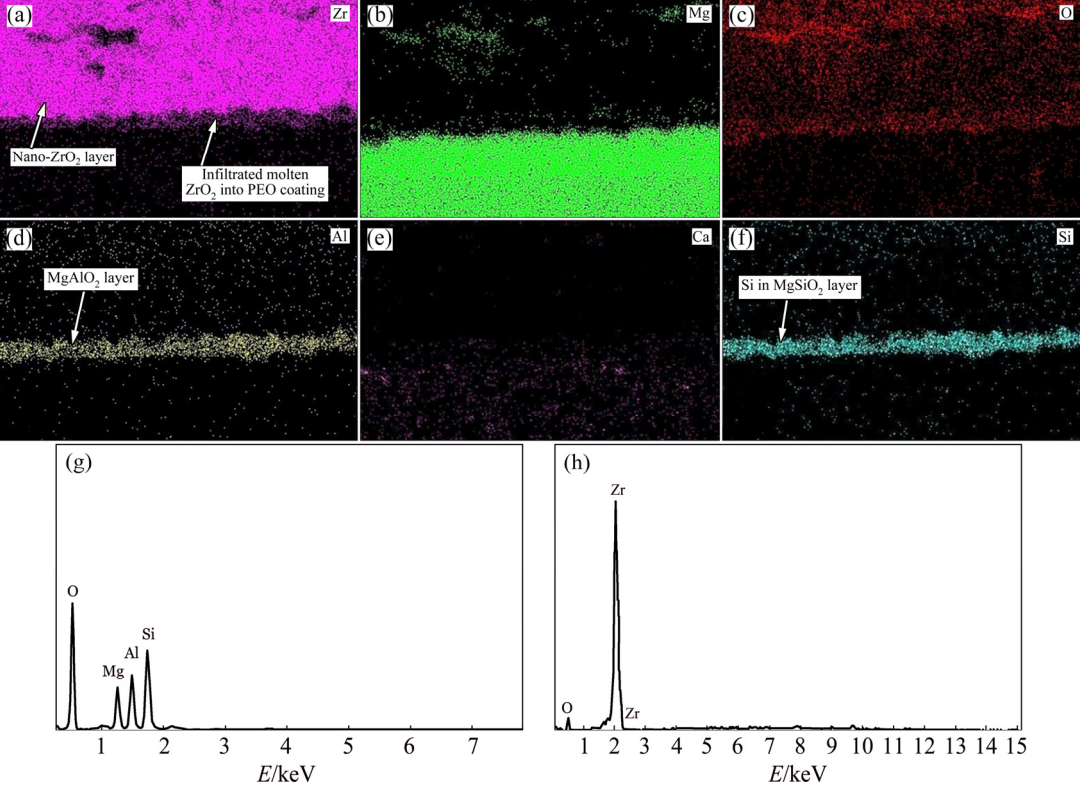


Fig. 3 EDX mapping from cross section of multilayered PEO/nanostructured ZrO<sub>2</sub> coated Mg alloy (a-f), EDX area from PEO layer surface (g) and from ZrO<sub>2</sub> layer surface (h)

elements in the multiphase PEO layer (see Figs. 3(g) and (h)).

Figures 4(a)–(d) demonstrate XRD patterns of bare Mg alloy, multiphase PEO layer, granulated  $ZrO_2$  powders and nanostructured  $ZrO_2$  layer, respectively. Figure 4(a) shows that the main phase of the alloy is  $\alpha$ -Mg with hexagonal close packed (HCP) crystalline structure. However, Mg<sub>2</sub>Ca phase was not identified, which is consistent with the previous studies [40]. In fact, Mg<sub>2</sub>Ca phase with HCP crystalline structure has a space group of  $P_{63}/mmc$  and the lattice parameters of a= 0.623 nm and c=1.012 nm. But, the size of the lattice parameters of this phase is two times larger than that of  $\alpha$ -Mg phase [41].

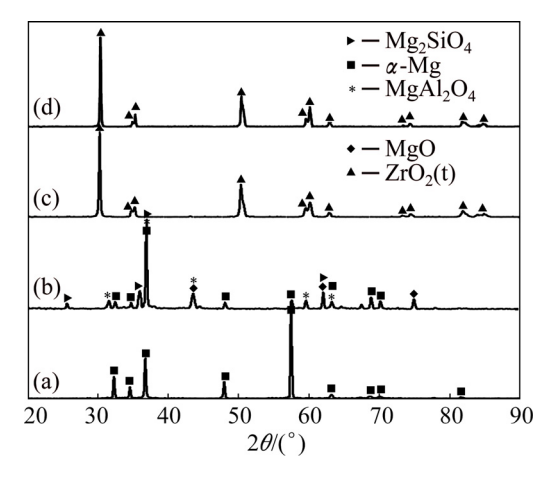


Fig. 4 XRD patterns of bare Mg alloy (a), multiphase PEO layer (b), granulated  $ZrO_2$  powders (c) and nanostructured  $ZrO_2$  layer (d)

The XRD pattern of the PEO coated Mg alloy (Fig. 4(b)) depicts that PEO coating is largely constituted by  $\alpha$ -Mg, MgAl<sub>2</sub>O<sub>4</sub>, MgO and Mg<sub>2</sub>SiO<sub>4</sub> phases. The existence of  $\alpha$ -Mg peaks (in XRD pattern of PEO coated sample) which have likely been extracted from Mg alloy surface originated from low thickness and loose microstructure of the PEO coatings. It is obviously seen that the produced coating is crystalline in nature. This observation may be related to the clear sharpness of all the diffracted peaks.

Figure 4(c) shows that nanostructured  $ZrO_2$  agglomerated powder is largely constituted by only non-transformable tetragonal phase. Figure 4(d) obviously indicates that nanostructured  $ZrO_2$  layer is mainly composed of non-transformable tetragonal  $ZrO_2$  phase which could originate from rapid solidification (quenching of the molten droplets) during air plasma spraying [34]. It is interesting to note that cooling rate of splats was reported to be  $10^7$  °C/s during APS process [36].

Vickers hardness tester (HVS-10) was employed to measure micro-hardness of treated and untreated

samples. This test was performed on the polished cross section of treated Mg alloys (from coating surface to the interface of Mg alloy/coating) at ten different places under a load of 150 g for 15 s and the average value was demonstrated (Fig. 5). Micro-hardness of Mg alloy is measured to be only HV 77.9. It is apparent that multiphase PEO coating is substantially able to develop micro-hardness of Mg alloy substrate (HV 300.5). Hence, inert multiphase PEO bond coat (with nearly rough surface) could afford needed micro-hardness for Mg alloy substrate to integrate with nanostructured ZrO<sub>2</sub> layer which could substantially increase the hardness to HV 740. It is expected that PEO/nanostructured ZrO<sub>2</sub> coating could remarkably enhance mechanical properties of the substrate.

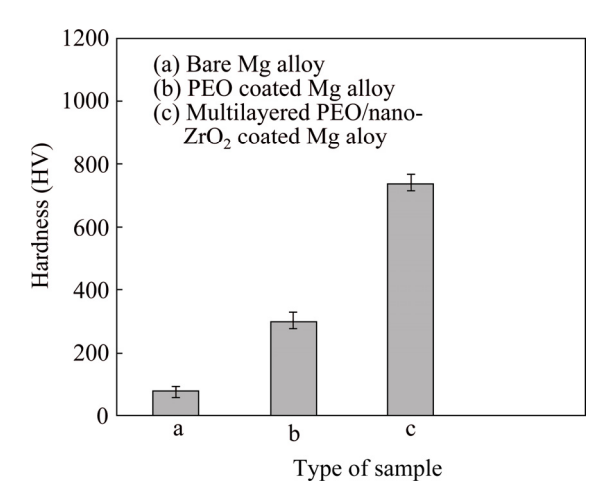
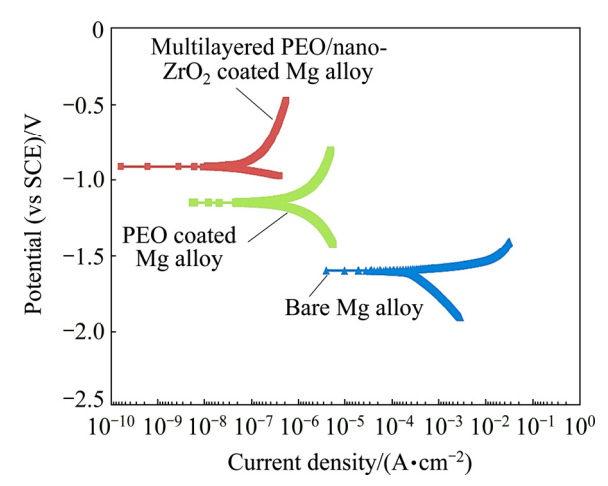


Fig. 5 Micro-hardness of coated and uncoated Mg alloys

#### 3.2 Electrochemical measurement

Figure 6 depicts the anodic and cathodic polarization curves of bare Mg alloy, multiphase PEO coated Mg alloy and PEO/nano-ZrO<sub>2</sub> coated Mg alloy in the SBF solution. The corrosion potentials ( $\varphi_{\text{corr}}$  vs SCE) of untreated Mg alloy, PEO coated Mg alloy and PEO/nanostructured ZrO<sub>2</sub> coated Mg alloy are –1601, –1148 and –912 mV, respectively. Thus, it is expected that Mg dissolution could remarkably be diminished by the PEO/nano-ZrO<sub>2</sub> coating with more positive corrosion potential.

It is visible that multiphase PEO coating has ability to decline the corrosion current density ( $J_{\rm corr}$ ) of substrate to 0.21  $\mu$ A/cm<sup>2</sup> which is lower than  $J_{\rm corr}$  of uncoated Mg alloy substrate (280.4  $\mu$ A/cm<sup>2</sup>). This statement has a direct relationship with inert nature and microstructure of the PEO coatings which can generally slow the transportation rate of the electrolyte in the PEO coated samples during corrosion. This phenomenon can mostly lessen  $J_{\rm corr}$  of PEO coated sample in aggressive electrolyte. However,  $J_{\rm corr}$  of PEO/ nanostructured ZrO<sub>2</sub> coated sample was noticeably declined to 0.062  $\mu$ A/cm<sup>2</sup>. In fact, the diffusion (penetration) of aggressive



**Fig. 6** Anodic and cathodic polarization curves of bare Mg alloy, multiphase PEO coated Mg alloy and multilayered PEO/nano-ZrO<sub>2</sub> coated Mg alloy in SBF solution

electrolyte (corrosive ions from the SBF solution) into the Mg alloy surface can substantially be postponed and suppressed by applying a compact, more uniform and slightly thicker PEO/ nanostructured ZrO<sub>2</sub> coating on metallic substrate. However, it is interesting to point out that single multiphase PEO layer (composed of stable oxide phases, particularly Mg<sub>2</sub>SiO<sub>4</sub> phase) is not able to substantially preserve Mg alloy in SBF solution. This mainly related the microstructural is to characteristics of the PEO coatings. nanostructured ZrO<sub>2</sub> coating (as top coat) on the multiphase PEO layer (as bond coat) would be able to increase considerably the corrosion protection performance of PEO layer on Mg alloy physiological solutions. This multiphase PEO layer is able to preserve Mg alloy from aggressive ion when it permits through from nanostructured ZrO2 top coat during corrosion.

Figures 7 and 8 demonstrate the EIS data (Nyquist and Bode plots) for the coated Mg alloys as well as bare Mg alloy in SBF solution. It is easily seen that both treated and untreated samples demonstrate a single capacitive loop at all high frequencies (Figs. 7(a) and (b)). This observed behavior was also seen in Mg samples coated with MAO/Ni-P coating and other types of multilayered coatings which also depicted one capacitive loop in their Nyquist curve although they had two or more layers [37–45]. However, single multiphase PEO coating and PEO/nano-ZrO<sub>2</sub> coating showed bigger diameter of capacitive loop compared with the bare Mg alloy.

It was reported that charge transfer resistance can ascertain the corrosion resistance of sample. Moreover, there was a direct relationship between charge transfer resistance and the diameter of the capacitive loop of Nyquist curve. Hence, preferable corrosion resistance of

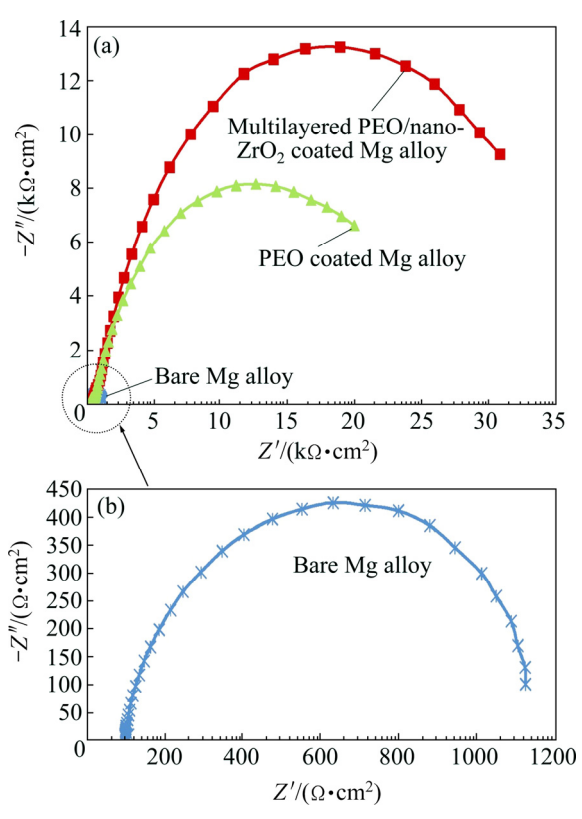


**Fig. 7** EIS data (Nyquist plots) for coated Mg alloys as well as bare Mg alloy in SBF solution

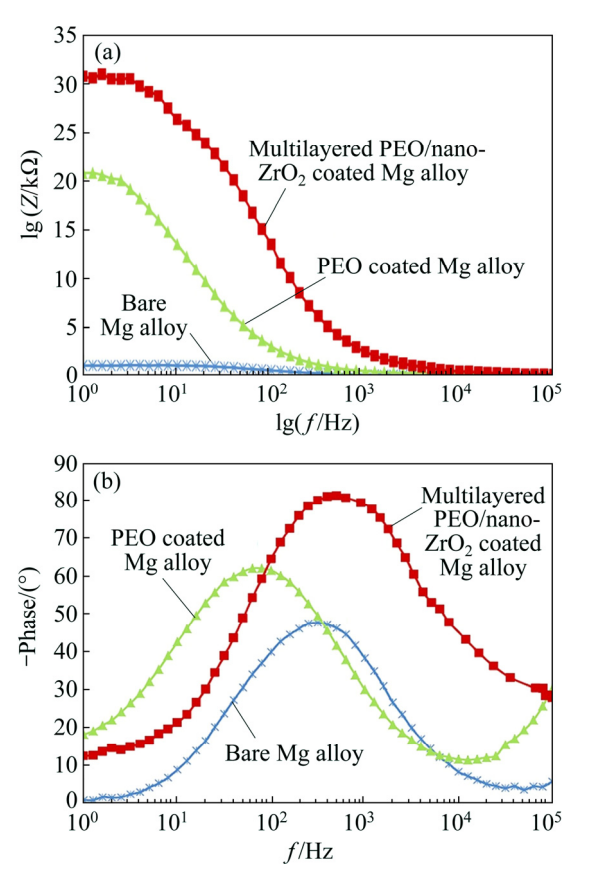


**Fig. 8** EIS data (Bode plots) for coated Mg alloys as well as bare Mg alloy in SBF solution: (a) Bode magnitude plots; (b) Bode phase angle plots

coated sample is in a direct connection with its greater charge transfer resistance and bigger diameter of its capacitive loop compared with those of uncoated sample [46,47]. Thus, charge transfer resistance ( $R_{\rm ct}$ ) of PEO/nano-ZrO<sub>2</sub> coated Mg alloy (30.830 k $\Omega$ ·cm²) is higher than that of multiphase PEO coated Mg alloy (19.941 k $\Omega$ ·cm²) and uncoated Mg alloy (1.124 k $\Omega$ ·cm²). In fact, excellent corrosion resistance of PEO/nano-ZrO<sub>2</sub> coating could be affected by low solubility, higher thickness and compactness of ZrO<sub>2</sub> coating as well as good corrosion resistance of multiphase PEO coating (as bond coat) on Mg alloy.

Bode magnitude plots and Bode phase plots are shown in Figs. 8(a) and (b), respectively. It is clearly seen that there is a direct relationship between impedance modulus (Z) at lower frequency (Fig. 8(a)) and charge transfer resistance ( $R_{\rm ct}$ ). This statement is in agreement with the previous investigations [48–50]. It is easily observed that impedance modulus of PEO/nano-ZrO<sub>2</sub> coated Mg alloy has noticeably been increased compared with Z of other samples at lower frequency (Fig. 8(a)). It was reported that phase angle and its broadening are two factors that can also

distinguish corrosion protective performance of the coatings [51,52]. The lowest and the highest values were found for untreated sample and PEO/ZrO2 coated sample, respectively (Fig. 8(b)). These lowest values may be related to the ultrathin formed oxide films (nanometric films) on bare Mg alloys which are very susceptible to the corrosive medias [46,53]. Hence, PEO/nano-ZrO<sub>2</sub> coating with the lowest anodic current density and the highest values of EIS data ( $R_{ct}$ , Z, phase angle) can effectively enhance the corrosion resistance of Mg alloy in physiological solutions. In fact, nano-ZrO<sub>2</sub> top coat can effectively seal PEO micro-defects and obstructing the transportation of corrosive ions in the PEO bond coat and followed by galvanic cell formation at the coating/Mg alloy interface [54,55]. According to these obtained results, the elaboration of corrosion process could be suggested by the following mechanism. Mg(OH)<sub>2</sub> formation can be expected at the PEO/Mg alloy interface (when electrolyte reaches interface of PEO/substrate through micro-pores in the coating) at the onset of corrosion. Dissolution and restructuring of Mg(OH)<sub>2</sub> can also be anticipated at the interface (freshly Mg surface) in this stage (see Fig. 9). Moreover, MgCl<sub>2</sub>

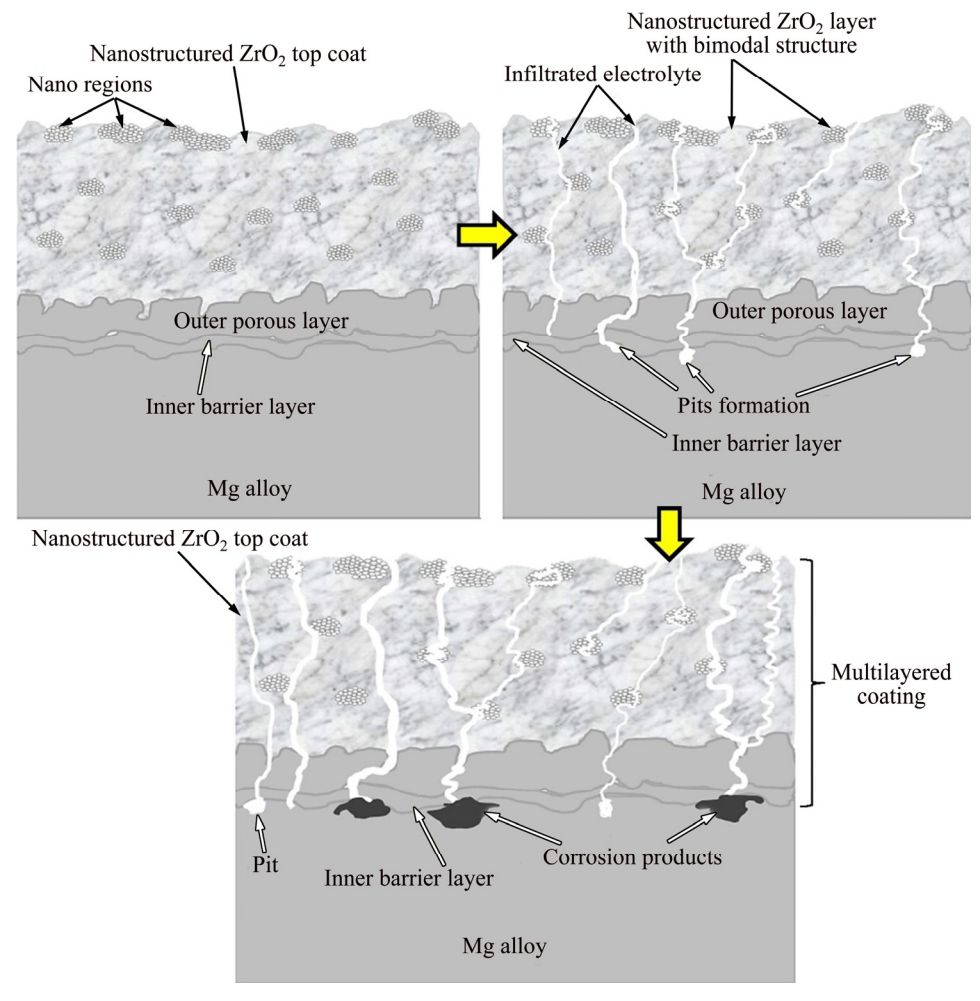


Fig. 9 Schematic illustration of electrochemical corrosion mechanism of multilayered PEO/nanostructured ZrO<sub>2</sub> coated Mg alloy in simulated body fluid solution

formation (substituting OH<sup>-</sup> by Cl<sup>-</sup>) with high solubility may locally dissolve the surface film and exposes freshly Mg surface to be re-corroded [6]. Mg dissolution followed by hydrogen formation (evolution) which could apply pressures on PEO layer and causes micro-cracks formation and coating separation are predicted in the subsequent stage [40,41,49,56]. However, nano-ZrO<sub>2</sub> top coat (with bimodal and compact structure [57]) which has completely sealed PEO bond coat is able to considerably prevent and delay aggressive ions transportation [58] (Fig. 9). Hence, PEO/nano-ZrO<sub>2</sub> coating can be considered as a good candidate to substantially enhance corrosion resistance of Mg alloy in the SBF solution.

### 3.3 Antibacterial activities of bare Mg alloy, PEO and PEO/nano-ZrO<sub>2</sub> coated Mg alloy

The antibacterial activities of the bare Mg alloy, multiphase PEO coated Mg alloy and PEO/nano-ZrO<sub>2</sub> coated Mg alloy were tested for *Escherichia coli* (Gram negative) bacteria via disc diffusion method (see Fig. 10). Less significant zone of inhibition can be detected under contact with bare Mg alloy. The inhibition zone diameter

increases after PEO and PEO/nano-ZrO2 coatings which indicated high antibacterial activity toward E. coli. The size of the inhibition zone was in the range of 2.5 mm for the PEO/nano-ZrO<sub>2</sub> coated samples whereas zones of inhibition was in the range of 1.6-1.2 mm for PEO coated and bare Mg alloy samples, respectively. Formation of a clear inhibition zone in the areas surrounding the surface of PEO/nano-ZrO2 coated Mg alloy further confirmed that the specimens have a great antibacterial activity against E. coli. Regarding antibacterial activity of multiphase PEO coated Mg alloy, the existence of micro-pores and micro-cracks on the surface of PEO layer, leading to the exposure of Mg substrate to the bacterial medium and thus maintaining its antibacterial performance because of its degradation and subsequent escalation in the pH value [59]. However, the main reason of good antibacterial performance of PEO/nano-ZrO<sub>2</sub> coated sample is attributed to the presence of ZrO<sub>2</sub> nanoparticles which decelerate E. coli growth as a result of E. coli membranes and thus escalate membrane permeability resulted in deposition of nanoparticles in the bacterial membrane and cytoplasmic areas of the cells [60].

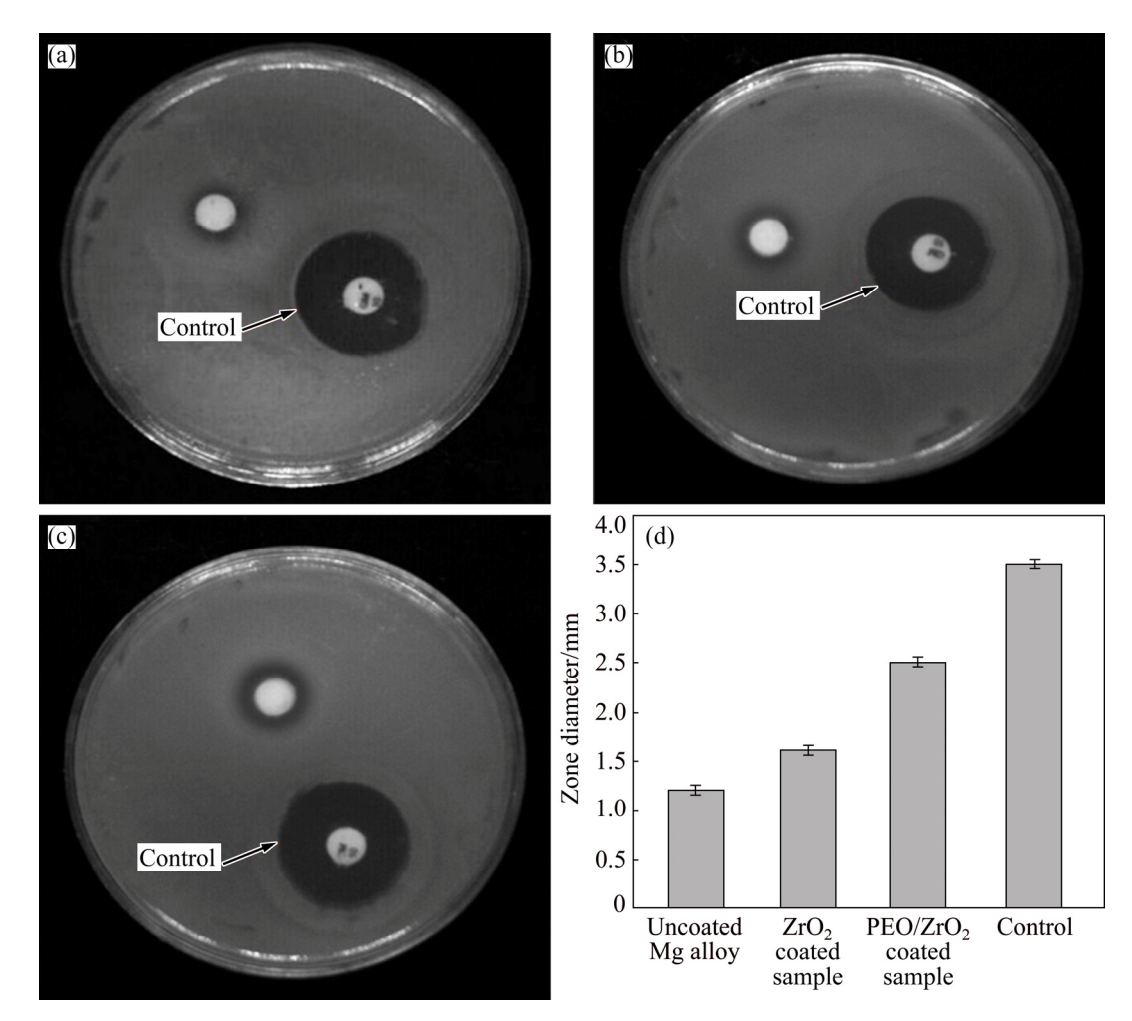


**Fig. 10** Inhibition zones of uncoated Mg alloy (a), PEO coated (b), PEO/nanostructured ZrO<sub>2</sub> coated samples (c) and growth inhibition zones of uncoated and coated samples against *E. coli* bacteria for 24 h (d)

#### 4 Conclusions

The results depict that nanostructured ZrO<sub>2</sub> top coat can easily be applied on the multiphase PEO (as bond coat) coated Mg alloy using APS method with the aid of compressed air. This case would lead to the considerable decrease in corrosion current density from 280.4 µA/cm<sup>2</sup>, for bare Mg alloy to 0.062 μA/cm<sup>2</sup> for the multilayered coating. In comparison with single multiphase PEO bond coat, the PEO/nanostructured ZrO2 coating shows higher charge transfer resistant ( $R_{ct}$ ), impedance modulus (Z) and phase angle. Antimicrobial study exhibits that multi-phase PEO coated and PEO/nano-ZrO2 coated Mg alloys show antibacterial activity, but PEO/nano-ZrO<sub>2</sub> coated sample presents better activity against E. coli. Nano-ZrO<sub>2</sub> top coat which has completely sealed PEO bond coat is able to considerably prevent and delay aggressive ions transportation. Hence, PEO/nano-ZrO<sub>2</sub> coating can be considered as a good candidate to substantially enhance corrosion resistance of biodegradable Mg alloy in SBF solution.

#### Acknowledgments

The authors would like to acknowledge the Universiti Teknologi Malaysia (UTM) for providing research facilities and financial support under Grants No: (1) UTM-Research University Grant (RUG) (Q.J130000.2524.16H35), and (2) Nippon Sheet Glass (NSG) R.J130000.7324.4B300.

#### References

- TSAI W T, SUN I W. Electro-deposition of aluminum on magnesium (Mg) alloys in ionic liquids to improve corrosion resistance [J].
  Corrosion Prevention of Magnesium Alloys, 2013: 393–413.
- [2] CHIU L H, CHEN C C, YANG C F. Improvement of corrosion properties in an aluminum-sprayed AZ31 magnesium alloy by a post-hot pressing and anodizing treatment [J]. Surface and Coatings Technology, 2005, 191: 181–187.
- [3] YUE T M, XIE H, LIN X, YANG H O, MENG G H. Solidification behavior in laser cladding of AlCoCrCuFeNi high-entropy alloy on magnesium substrates [J]. Journal of Alloys and Compounds, 2014, 587: 588–593.
- [4] DAROONPARVAR Mohammadreza, YAJID M A M, YUSOF N M, BAKHSHESHI-RAD. Hamidreza, fabrication and properties of triplex NiCrAlY/nano Al<sub>2</sub>O<sub>3</sub>·13%TiO<sub>2</sub>/nano TiO<sub>2</sub> coatings on a magnesium alloy by atmospheric plasma spraying method [J]. Journal of Alloys and Compounds, 2015, 645: 450–466.
- [5] DAROONPARVAR M, YAJID M A M, YUSOF N M, BAKHSHESHI-RAD. Hamidreza, Preparation and corrosion resistance of a nanocomposite plasma electrolytic oxidation coating on Mg-1%Ca alloy formed in aluminate electrolyte containing titania nano-additives [J]. Journal of Alloys and Compounds, 2016, 688: 841-857.
- [6] CUI Xue-jun, YANG Rui-song, LIU Chun-hai, YU Zu-xiao, LIN Xiu-zhou. Structure and corrosion resistance of modified micro-arc oxidation coating on AZ31B magnesium alloy [J]. Transactions of

- Nonferrous Metals Society of China, 2016, 26: 814-821.
- [7] WANG Shu-yan, XIA Yong-ping. Micro arc oxidation coating fabricated on AZ91D Mg alloy in an optimized dual electrolyte [J]. Transactions of Nonferrous Metals Society of China, 2013, 23: 412–419.
- [8] BAKHSHESHI-RAD H, HAMZAH E, KAHRIZANGI E, DAROONPARVAR M, MEDRAJ M. Fabrication and characterization of hydrophobic micro are oxidation/poly-lactic acid duplex coating on biodegradable Mg-Ca alloy for corrosion protection [J]. Vacuum, 2016, 125: 185–188.
- [9] FAN Xi-zhi, WANG Ying, ZOU-Bing-lin, GU Li-jian, HUANG Wen-zhi, CAO Xue-qiang. Preparation and corrosion resistance of MAO/Ni-P composite coat on Mg alloy [J]. Applied Surface Science, 2013, 277: 272–280.
- [10] SHI P C, NG W F, WONG M H, CHENG F T. Improvement of corrosion resistance of pure magnesium in Hanks' solution by micro arc oxidation with sol-gel titanium dioxide sealing [J]. Journal of Alloys and Compounds 2009, 469: 286–292.
- [11] RYU Hyun-Sam, PARK Dong-Soo, HONG Seong-Hyeon. Improved corrosion protection of AZ31 magnesium alloy through plasma electrolytic oxidation and aerosol deposition duplex treatment [J]. Surface and Coatings Technology, 2013, 219: 82–87.
- [12] ZHAO Quan-ming, GUO Xiong, DANG Qian-xiao, HAO Jian-min, LAI Jiang-hua, WANG Kun-zheng. Preparation and properties of composite MAO/ECD coatings on magnesium alloy [J]. Colloids and Surfaces B: Biointerfaces, 2013,102: 321–326.
- [13] LIMA R S, MARPLE B R. Thermal spray coatings engineered from nanostructured ceramic agglomerated powders for structural, thermal barrier and biomedical applications: A review [J]. Journal of Thermal Spray Technology, 2007, 16: 40–63.
- [14] FAN Xi-zhi, LIU Yang-jia, XU Zhen-hua, WNG Ying, ZOU Bing-lin, GU Li-jian, WANG Chun-jie, CHEN Xiao-long, KHAN Z S, YANG Dao-wu, CAO Xue-qiang. Preparation and characterization of 8YSZ thermal barrier coatings on rare earth-magnesium alloy [J]. Journal of Thermal Spray Technology, 2011, 20: 948–957.
- [15] LI Chong-gui, WANG You, WAN Shi, GUO Li-xin. Laser surface remelting of plasma-sprayed nanostructured Al<sub>2</sub>O<sub>3</sub>-13wt%TiO<sub>2</sub> coatings on magnesium alloy [J]. Journal of Alloys and Compounds, 2010, 503: 127-132.
- [16] FAN Xi-zhi, ZOU Bing-lin, GUA Li-jian, WANGA Chun-jie, WANG Ying, HUANG Wen-zhi, ZHU Ling, CAO Xue-qiang. Investigation of the bond coats for thermal barrier coatings on Mg alloy [J]. Applied Surface Science, 2013, 265: 264–273.
- [17] BAKHSHESHI-RAD H, HAMZAH E, ISMAIL A F, DAROONPARVAR M, KASIRI A M, JABBARZARE S, MEDRAJ M. Microstructural, mechanical properties and corrosion behavior of plasma sprayed NiCrAlY/nano-YSZ duplex coating on Mg-1.2Ca-3Zn alloy [J]. Ceramics International, 2015, 41: 15272-15277.
- [18] BAKHSHESHI-RAD H, ABDELLAHI A, HAMZAH E, DAROONPARVAR M, RAFIEI M [J]. Introducing a composite coating containing CNTs with good corrosion properties: Characterization and simulation [J]. RSC Advances, 2016, 6: 108498–108512.
- [19] DAROONPARVAR M, YAJID M A M, YUSOF N M, BAKHSHESHI-RAD H, Improvement of thermally grown oxide layer in thermal barrier coating systems with nano alumina as third layer [J]. Transactions of Nonferrous Metals Society of China, 2013, 23: 1322-1333.
- [20] DAROONPARVAR M, YAJID M A M, YUSOF N M, BAKHSHESHI-RAD H, ESAH H. Effect of Y<sub>2</sub>O<sub>3</sub> stabilized ZrO<sub>2</sub> coating with tri-model structure on bi-layered thermally grown oxide evolution in nano thermal barrier coating systems at elevated temperatures [J]. Journal of Rare Earths, 2014, 32: 57–77.

- [21] DAROONPARVAR M, YAJID M A M, HUSSAIN M. S, The role of formation of continues thermally grown oxide layer on the nanostructured NiCrAIY bond coat during thermal exposure in air [J]. Applied Surface Science, 2012, 261: 287–297.
- [22] DAROONPARVAR M, YAJID M A M, YUSOF N M, BAKHSHESHI-RAD H, HAMZAH E, NAZOKTABAR. Investigation of three steps of hot corrosion process in  $Y_2O_3$  stabilized ZrO<sub>2</sub> coatings including nano zones [J]. Journal of Rare Earths, 2014, 32: 989–1002.
- [23] DING C, LIU X. Microstructure and properties of plasma sprayed nano-structural ZrO<sub>2</sub> coatings [J]. Nanoelectronics Conference, 2010: 12–13.
- [24] YANG Yong, YAN Dian-ran, DONG Yan-chun, CHEN Xue-guang, WANG Lei, CHU Zhen-hua, ZHANG Jian-xin, HE Ji-ning. Preparing of nanostructured Al<sub>2</sub>O<sub>3</sub>–ZrO<sub>2</sub>–TiO<sub>2</sub> composite powders and plasma sprayed nanostructured composite coatings [J]. Vacuum, 2013, 96: 39–45.
- [25] BAIA Y, HANA Z H, LI H Q, XUA C, XU Y L, WANG Z, DING C H, YANG J F. High performance nanostructured ZrO<sub>2</sub> based thermal barrier coatings deposited by high efficiency supersonic plasma spraying [J]. Applied Surface Science, 2011, 257: 7210–7216.
- [26] DAROONPARVAR M, YAJID M A M, YUSOF N M, HUSSAIN M S. Improved thermally grown oxide scale in air plasma sprayed NiCrAlY/Nano-YSZ coatings [J]. Journal of Nanomaterials, 2013, 2013(1): 87–89.
- [27] BAKHSHESHI-RAD H, HAMZAH E, LOW H T, KASIRI-ASGARANI, FARAHANY S, AKBARI E, CHO M H. Fabrication of biodegradable Zn-Al-Mg alloy: Mechanical properties, corrosion behavior, cytotoxicity and antibacterial activities [J]. Materials Science and Engineering C, 2017, 73: 215-219
- [28] GNEDENKOV S V, SINEBRYUKHOV S L, MASHTALYAR D V, IMSHINETSKIY I M, GNEDEKOV A S, SAMOKHIN A V, TSVETKOV Y V. Protective composite coatings obtained by plasma electrolytic oxidation on magnesium alloy MA8 [J]. Vacuum, 2015, 120: 107–114.
- [29] DURDU S, BAYRAMOGLU S, EMIRTAS D A, USTA M, UCISIK H A. Characterization of AZ31 Mg alloy coated by plasma electrolytic oxidation [J]. Vacuum, 2013, 88: 130–133.
- [30] ZHANG Lei, ZHANG Jun-qing, CHEN Cheng-fu, GU Yan-hong. Advances in micro arc oxidation coated AZ31 Mg alloys for biomedical applications [J]. Corrosion Science, 2015, 91: 116–122.
- [31] SREEKANTH D, RUMESHBABU N, VENKATESWARU V. Effect of various additives on morphology and corrosion behavior of ceramic coatings developed on AZ31 magnesium alloy by plasma electrolytic oxidation [J]. Ceramics International, 2012, 38: 4607–4615.
- [32] CHARLES J, ENGBER G, ERNEST H, ZHEMS H. Thermal Expansion of Al<sub>2</sub>O<sub>3</sub>, BeO, MgO, B<sub>4</sub>C, SiC, and TiC Above 1000 °C [J]. Journal of the American Ceramic Society, 2006, 42: 300–305.
- [33] FIQUET G, RICHET P, MONTAGNAC G. High-temperature thermal expansion of lime, periclase, corundum and spinel [J]. Physics and Chemistry of Minerals, 1999, 27: 103–111.
- [34] DAROONPARVAR M. Effects of bond coat and top coat (including nano zones) structures on morphology and type of formed transient stage oxides at pre-heat treated nano NiCrAIY/nano ZrO<sub>2</sub>-8% Y<sub>2</sub>O<sub>3</sub> interface during oxidation [J]. Journal of Rare Earths, 2015, 33: 983-994.
- [35] LIMA R S, DIMITRIEVSKA S, BUREAU M N, MARPLE B R, PETIT A, MWALE F, ANTONIOU J. HVOF-sprayed nano TiO-HA coatings exhibiting enhanced biocompatibility [J]. Journal of Thermal Spray Technology, 2010, 19: 336–347.
- [36] GHASEMI R, SHOJA-RAZAVI R, MOZAFARINIA R, JAMALI H. The influence of laser treatment on thermal shock resistance of

- plasma-sprayed nanostructured yttria stabilized zirconia thermal barrier coatings [J]. Ceramics International, 2014, 40: 347–355.
- [37] ZHANG C L, ZHANG F, SONG L, ZENG R C, LI S Q, HAN E H. Corrosion resistance of a superhydrophobic surface on micro-are oxidation coated Mg-Li-Ca alloy [J]. Journal of Alloys and Compounds, 2017, 728: 518-826.
- [38] WU Guo-song, SHANAGHI A, ZHAO Ying, ZHANG Xu-ming, XU Rui-zhen, WU Zheng-wei, LI Guang-yao, CHU P K. The effect of interlayer on corrosion resistance of ceramic coating/Mg alloy substrate in simulated physiological environment [J]. Surface and Coating Technology, 2012, 206: 4892–4898.
- [39] GUO Xing-wu, WANG Shao-hua, GONG Jia, GUO Jia-cheng, PENG Li-ming, DING Wen-jiang. Characterization of highly corrosion-resistant nanocrystalline Ni coating electro deposited on Mg-Nd-Zn-Zr alloy from a eutectic-based ionic liquid [J]. Applied Surface Science, 2014, 313: 711-719.
- [40] PAK Sung-Nam, JIANG Zhao-hua, YAO Zhong-ping. Fabrication of environmentally friendly anti-corrosive composite coatings on AZ31B Mg alloy by plasma electrolytic oxidation and phytic acid/3-aminopropyltrimethoxysilane post treatment [J]. Surface and Coating Technology, 2017, 325: 579–587.
- [41] GUO Lian, ZHANG Fen, SONG Liang, ZENG Rong-chang. Corrosion resistance of ceria/polymethyltrimethoxysilane modified magnesium hydroxide coating on AZ31 magnesium alloy [J]. Surface and Coating Technology, 2017, 328: 121–133.
- [42] EZHILSELVI V, BALARAJU J N, SUBRAMANIAN S. Chromate and HF free pretreatment for MAO/electroless nickel coating on AZ31B magnesium alloy [J]. Surface and Coating Technology, 2017, 325: 270-276
- [43] XI Zhong-xian, TAN Cui, XU Lan, YANG Na, LI Qing. Preparation of novel functional Mg/O/PCL/ZnO composite biomaterials and their corrosion resistance [J]. Applied Surface Science, 2105, 351: 410–415.
- [44] LI Xia, WENG Zheng-yang, YUAN Wei, LUO Xian-zi, WONG Hoi-man, LIU Xiang-mei, WU Shui-lin, YEUNG K W K, ZHENG Yu-feng, CHU Paul K. Corrosion resistance of dicalcium phosphate dihydrate/poly(lactic-co-glycolic acid) hybrid coating on AZ31 magnesium alloy [J]. Corrosion Science, 2016, 102: 209–221.
- [45] CUI Lan-yue, XU Ji, LU Na. In vitro corrosion resistance and antibacterial properties of layer-by-layer assembled chitosan/poly-Lglutamic acid coating on AZ31 magnesium alloys [J]. Transactions of Nonferrous Metals Society of China, 2017, 27: 1081–1086.
- [46] WANG S Y, SI N S, XIA Y P, LIU L. Influence of nano-SiC on microstructure and property of MAO coating formed on AZ91D magnesium alloy [J]. Transaction of nonferrous Metals Society of China, 2015, 25: 1926–1934.
- [47] PING W, JIANPING L, YOUNCHUN G, ZHONG Y. Growth process and corrosion resistance of ceramic coatings of micro-arc oxidation on Mg-Gd-Y magnesium alloys [J]. Journal of Rare Earths, 2010, 28: 798-802.
- [48] WANG Y, WANG X. Role of β phase during micro are oxidation of Mg alloy AZ91D and corrosion resistance of the oxidation coating [J]. Journal of Materials Science Technology, 2013, 29: 1129–1133.
- [49] DAROONPARVAR M, YAJID M A M, YUSOF N M, BAKHSHESHI-RAD H, HAMZAH E, KAMALI H A. Microstructural characterization and corrosion resistance evaluation of nanostructured Al and Al/AlCr coated Mg–Zn–Ce–La alloy [J]. Journal of Alloys and compounds, 2014, 615: 657–671.
- [50] DAROONPARVAR M, YAJID M A M, YUSOF N M, BAKHSHESHI-RAD H, HAMZAH E, MARDANIKIVI T. Deposition of duplex MAO layer/nanostructured titanium dioxide composite coatings on Mg-1%Ca alloy using a combined technique of air plasma spraying and micro arc oxidation [J]. Journal of Alloys and Compounds, 2015, 649: 591-605.

- [51] MANDAL M, MOON A P, DEO G, MENDIS C L, MONDAL K. Corrosion behavior of Mg-2.4Zn alloy micro-alloyed with Ag and Ca [J]. Corrosion Science, 2014, 78: 172-182.
- [52] DEJIU S, HAOJIE M, CHANGHONG G, JINGRUI C, GUOLONG L. Effect of cerium and lanthanum additives on plasma electrolytic oxidation of AZ31 magnesium alloy [J]. Journal of Rare Earths, 2013, 31: 1208–1213
- [53] NIU Y, CUI R, HE Y, YU Z. Wear and corrosion behavior of Mg-Gd-Y-Zr alloy treated by mixed molten-salt bath [J]. Journal of Alloys and Compounds, 2014, 610: 294-300.
- [54] CUI X J, LIN X Z, LIU C H. Fabrication and corrosion resistance of a hydrophobic micro-arc oxidation coating on AZ31 Mg alloy [J]. Corrosion Science, 2015, 90: 402–412.
- [55] SURMENEVA M A, SURMENEV R A. Microstructure characterization and corrosion behavior of a nano-hydroxyapatite coating deposited on AZ31 magnesium alloy using radio frequency magnetron sputtering [J]. Vacuum, 2015, 117: 60–62.
- [56] DAROONPARVAR M, MAT YAJID M A, KUMAR GUPTA R, MOHD YUSOF N, BAKHSHESHI-RAD H R, GHANDVAR H. Investigation of corrosion protection performance of multiphase PEO (Mg<sub>2</sub>SiO<sub>4</sub>, MgO, MgAl<sub>2</sub>O<sub>4</sub>) coatings on Mg alloy formed in aluminate-silicate-based mixture electrolyte [J]. Protection of Metals

- and Physical Chemistry of Surfaces, 2018, 54: 425-441.
- [57] DAROONPARVAR M, MAT YAJID M A, KAY C M, BAKHSHESHI-RAD H, KUMAR GUPTA R, MOHD YUSOF N, GHANDVAR H, ARSHAD A, MOHD ZULKIFLI I S. Effects of Al<sub>2</sub>O<sub>3</sub> diffusion barrier layer (including Y-containing small oxide precipitates) and nanostructured YSZ top coat on the oxidation behavior of HVOF NiCoCrAITaY/APS YSZ coatings at 1100 °C [J]. Corrosion Science, 2018, https://doi.org/10.1016/j.corsci.2018.07. 013.
- [58] DAROONPARVAR M, MAT YAJID M A, BAKHSHESHI-RAD H R, YUSOF N M, IZMAN S, HAMZAH E, ABDUL KADIR M R. Corrosion resistance investigation of nanostructured Si-and Si/TiO<sub>2</sub>-coated Mg alloy in 3.5% NaCl solution [J]. Vacuum, 2014, 108: 61-65
- [59] REN L, LIN X, TAN L, YANG K. Effect of surface coating on antibacterial behavior of magnesium based metals [J]. Materials Letters, 2011, 65: 3509–3511.
- [60] GOWRI S, RAJIV R G, SUNDRARAJAN M. Structural, optical, antibacterial and antifungal properties of zirconia nanoparticles by biobased protocol [J]. Journal of Materials Science Technology, 2014, 30(8): 782-790.

### 新型 PEO/纳米结构 ZrO<sub>2</sub> 镁合金涂层的 抗菌活性及腐蚀行为

Mohammadreza DAROONPARVAR<sup>1,2</sup>, Muhamad Azizi MAT YAJID<sup>1</sup>, Rajeev KUMAR GUPTA<sup>2</sup>, Noordin MOHD YUSOF<sup>1</sup>, Hamid Reza BAKHSHESHI-RAD<sup>1,3</sup>, Hamidreza GHANDVAR<sup>1</sup>, Ehsan GHASEMI<sup>4</sup>

1. Department of Materials, Manufacturing and Industrial Engineering,

Faculty of Mechanical Engineering, Universiti Teknologi Malaysia, 81310 Johor Bahru, Johor, Malaysia;

2. Department of Chemical and Biomilecular Engineering, Corrosion Engineering Program,

The University of Akron, Akron, OH-44325, United States of America;

- 3. Advanced Materials Research Center, Department of Materials Engineering,
  - Najafabad Branch, Islamic Azad University, Najafabad, Iran;
- 4. Department of Clinical Sciences, Faculty of Veterinary Medicine, University of Tehran, Tehran, Iran

摘 要:为了增强镁合金的耐腐蚀性和抗菌活性,先采用等离子体电解氧化(PEO)在镁合金上制备一层结合层,再用空气等离子喷涂(APS)制备纳米结构 ZrO<sub>2</sub>表面涂层。采用电化学试验研究涂层样品的腐蚀行为,采用琼脂扩散法对其进行大肠杆菌病原菌抑菌活性评价,并与无涂层样品进行对比。与 PEO 涂层和无涂层镁合金相比,PEO/纳米 ZrO<sub>2</sub> 涂层样品的腐蚀电流密度最低,电荷传递阻力最高,相位角和阻抗模量最高。PEO 结合涂层被纳米 ZrO<sub>2</sub> 表面涂层完全密封,能够显著延缓侵蚀性离子向镁合金表面迁移,显著提高镁合金在模拟体液(SBF)中的耐蚀性。此外,PEO/纳米 ZrO<sub>2</sub> 涂层的抗菌活性也高于 PEO 涂层和无涂层镁合金,这是由于 ZrO<sub>2</sub> 纳米颗粒通过作用于细胞膜而降低了大肠杆菌的生长速率。

关键词: 镁合金; 陶瓷; 涂层材料; 显微组织; 扫描电镜